aluminum alums including a deuterate and a selenate.[4] The symmetric aluminum–water stretch $\nu_1(M^{III}–OH_2)$ occurs between 511 and 544 cm^{-1}, consistent with our assignment of the antisymmetric stretch ν_3 at the higher frequency of ~590 cm^{-1}. Our assignment of ν_3 does not agree with those made from infrared studies[1,3] of cesium and potassium aluminum alums. Furthermore, our assignments of the external $M^{III}–OH_2$ modes are not in agreement with a low-temperature infrared study[1] or some aspects of the Raman study mentioned above.[4] We plan to record low-temperature infrared and Raman spectra in an attempt to resolve these differences. However, there now seems little doubt about the correctness of our assignments of the infrared active metal–ligand stretching frequencies which lie between 500 and 600 cm^{-1} for these $M(H_2O)_6^{3+}$ complexes.

Acknowledgment. We thank Dr. Noel Cant and Peter Matthews of Macquarie University, Sydney, for use of the Perkin-Elmer Model 580 spectrometer, Dr. Mick Withers of the University of New South Wales, Sydney, for the use of a cryostat, and Dr. David M. Adams for helpful discussions.

Registry No. $CsAl(SO_4)_2·12H_2O$, 7784-17-0; $CsCo(SO_4)_2·12H_2O$, 19004-44-5; $CsCr(SO_4)_2·12H_2O$, 15363-19-6; $CsV(SO_4)_2·12H_2O$, 29931-99-5; $CsTi(SO_4)_2·12H_2O$, 16482-51-2; $CsFe(SO_4)_2·12H_2O$, 24389-85-3; $KAl(SO_4)_2·12H_2O$, 7784-24-9; $NH_4Al(SO_4)_2·12H_2O$, 7784-26-1; $KCr(SO_4)_2·12H_2O$, 7788-99-0; $NH_4Cr(SO_4)_2·12H_2O$, 10022-47-6; $Al^{III}(H_2O)_6$, 15453-67-5; $Co^{III}(H_2O)_6$, 15275-05-5; $Cr^{III}(H_2O)_6$, 14873-01-9; $V^{III}(H_2O)_6$, 21374-21-0; $Ti^{III}(H_2O)_6$, 17524-20-8; $Fe^{III}(H_2O)_6$, 15377-81-8.

Contribution from the School of Chemical Sciences, University of East Anglia, Norwich, United Kingdom, the Laboratory for Chemistry and Technology of the Radioelements of CNR, Padua, Italy, the Institute of Inorganic Chemistry of the University of Turin, Turin, Italy, and the Department of Industrial and Engineering Chemistry of the Swiss Federal Institute of Technology, ETH, Zurich, Switzerland

Comparative Infrared and Raman Spectroscopic ν(CO) Study of $Ru_3(CO)_{12}$, $Os_3(CO)_{12}$, Their Mixed Crystals, and the Mixed Triangulo Cluster Carbonyls $Ru_2Os(CO)_{12}$ and $RuOs_2(CO)_{12}$[1a]

GIOVANNI A. BATTISTON,[1b] GYÖRGY BOR,*[1c] URS K. DIETLER,[1c] SIDNEY F. A. KETTLE,*[1d] ROSANNA ROSSETTI,[1e] GINO SBRIGNADELLO,*[1b] and PIER LUIGI STANGHELLINI[1e]

Received September 7, 1979

High-resolution infrared and Raman spectra ν(CO) of the species $M_nM'_{3-n}(CO)_{12}$ (M, M′ = Ru, Os; n = 0, 1, 2, or 3) are reported. The species $Ru_2Os(CO)_{12}$ and $RuOs_2(CO)_{12}$ were, for the first time, prepared in a spectroscopically pure state for these studies. Data on ^{13}CO-enriched $Ru_3(CO)_{12}$ and $Os_3(CO)_{12}$ are also presented. A detailed ν(CO) vibrational analysis, using the rotational parameter method, has been performed on $Ru_3(CO)_{12}$, where overtone and intensity data have been used to augment fundamental frequencies and enable a definitive assignment. Intensity data were also used in the analysis on $Os_3(CO)_{12}$; the analyses of the Ru_2Os and $RuOs_2$ species used fundamental frequency data only. The average CO force constant has the same value (16.66 mdyn/Å) for each of the four compounds. Further, in this series individual equatorial and axial CO stretching force constants are characteristic of the metal atom involved and almost independent of the particular chemical species. All geminal interaction constants increase regularly from $Ru_3(CO)_{12}$ to $Os_3(CO)_{12}$, contributing, in part, to the spread in frequencies observed in passing from the triruthenium to the triosmium compound. The vibrational coupling between CO groups on different metal atoms is very significant so that it is clearly inappropriate to use a local symmetry approach to the analysis of the ν(CO) spectra of these compounds.

Introduction

During the past 15 years there have been many detailed studies of the vibrational spectra of metal carbonyls and their derivatives in the ν(CO) region. Although the majority of these have been confined to monomeric species, some detailed analyses have also been carried out in bi- and polynuclear carbonyls.[2] Some of us have recently reported detailed infrared studies of some tri- and tetranuclear species which have indicated that the combined use of frequency, band intensity, and isotopic data enables a definitive analysis to be carried out.[3,4] These studies have revealed that within a CO-factored force field, interaction constants between CO groups on adjacent atoms can be of the same order of magnitude as those between geminal CO groups. This observation is pertinent to the question of the extent of correlation of the motion between carbonyl groups on a metal surface, a topic of relevance to the understanding of the metal-surface-catalyzed reactions of CO.

The present paper is concerned with a detailed vibrational study of the trimetallo dodecacarbonyls of basic D_{3h} symmetry. The complex nature of the problems encountered in this work required for their solution the use of a variety of techniques, a situation which stimulated collaboration between several groups. The present paper is the product of the combined efforts of four laboratories; some of the more specific results obtained and the methods of analysis used are the subject of separate papers.

Vibrational spectroscopic studies on the triruthenium and triosmium dodecacarbonyls have been reported rather sporadically over the past few years; studies on $Os_3(CO)_{12}$ have been more common than those on its ruthenium analogue. The first, rather sketchy, report was that of Beck and Lottes,[5] but the paper of Huggins, Flitcroft, and Kaesz,[6] describing an infrared study of $Os_3(CO)_{12}$, was the first paper in which band assignments were made. Although, as we shall show, these assignments were correct on important points, the fact that

(1) (a) To be considered as part 20 of the series "Solid-State Studies" by S. F. A. Kettle and co-workers and part 22 of the series "Infrared Spectroscopic Studies of Metal Carbonyl Compounds" by G. Bor and co-workers. For parts 19 and 21, respectively, see ref 16 and 30. (b) Laboratory for Chemistry and Technology of the Radioelements of CNR. (c) Swiss Federal Institute of Technology, ETH. (d) University of East Anglia. (e) University of Turin.

(2) For reviews see: (a) M. L. Haines and M. H. B. Stiddard, *Adv. Inorg. Chem. Radiochem.*, **12**, 53 (1969); (b) P. S. Braterman, "Metal Carbonyl Spectra", Academic Press, London, New York, San Francisco, 1975; (c) P. S. Braterman, *Struct. Bonding (Berlin)*, **26**, 1 (1976); (d) S. F. A. Kettle, *Top. Curr. Chem.*, **71**, 111 (1977).

(3) G. Bor, G. Sbrignadello, and F. Marcati, *J. Organomet. Chem.*, **46**, 357 (1972).

(4) G. Bor, G. Sbrignadello, and K. Noack, *Helv. Chim. Acta*, **58**, 815 (1975).

(5) W. Beck and K. Lottes, *Chem. Ber.*, **94**, 2578 (1961).

(6) D. K. Huggins, N. Flitcroft, and H. D. Kaesz, *Inorg. Chem.*, **4**, 166 (1965).

0020-1669/80/1319-1961$01.00/0

the analysis was performed on the basis of a local C_{2v} symmetry, with the consequent neglect of all interactions between CO vibrators attached to different osmium atoms, means that the numerical values of the approximate force constants obtained by these authors are hardly meaningful since it is now clear that the local symmetry assumption is invalid.

Quicksall and Spiro[7] proposed a somewhat different assignment of the C–O stretching fundamentals on the basis of a study which included not only the Raman spectra of both $Os_3(CO)_{12}$ and $Ru_3(CO)_{12}$ in the crystalline state but also IR spectra recorded as KBr pellets. It is now clear that extensive correlation field splitting effects occur in the ν(CO) vibrational spectra of all crystalline metal carbonyls containing a high density of terminal CO groups. Such splittings would be expected for the trimetal dodecacarbonyls, an expectation which makes Quicksall and Spiro's neglect of possible correlation field effects suspect, and with it their analysis. It has to be recognized, however, that the emphasis of their paper was on the metal–metal frequencies as was also that of the paper of Hartley, Kilty, and Ware[8] and that for these modes correlation field effects seem to be absent.

In addition to a KBr infrared spectrum, a fingerprint infrared spectrum of $Ru_3(CO)_{12}$ in cyclohexane solution was reported by Yawney and Stone,[9] a report which seems to be the first one of a solution spectrum of this compound. The IR spectrum of $Ru_3(CO)_{12}$ has been described also in a low-temperature matrix study.[10]

That the triruthenium and triosmium compounds have analogous structures, of D_{3h} symmetry, has been known since the X-ray analyses of Corey and Dahl[11] on $Os_3(CO)_{12}$ and of Mason and Rae[12] on $Ru_3(CO)_{12}$. Recently both structures have been refined by Churchill et al.[13] Despite the high symmetry assumed for the isolated molecule and almost seen in the X-ray studies, the fact that each molecule occupies a C_1 site in the crystal lattice places a further uncertainty against data obtained from crystalline samples since site symmetry splitting of degenerate modes may occur as may also unexpected coupling and intensity stealing phenomena.[14]

The present study contains several aspects. High-resolution solution infrared spectra are reported for the species $Os_3(CO)_{12}$ and $Ru_3(CO)_{12}$ in the C–O stretching region.[15] The ν(CO) overtone/combination infrared spectrum of $Ru_3(CO)_{12}$ is also reported and used in our assignments. In addition, high-resolution infrared and Raman spectra obtained from crystalline samples (the infrared as KBr disks) are also reported together with, where appropriate, data on mixed crystals of general composition $[Os_3(CO)_{12}]_{1-x}[Ru_3(CO)_{12}]_x$, where $0 < x < 1$. Such studies help in detecting features originating in intermolecular vibrational coupling.[17] Further, the spectra of ^{13}CO-enriched species have been recorded as have those of

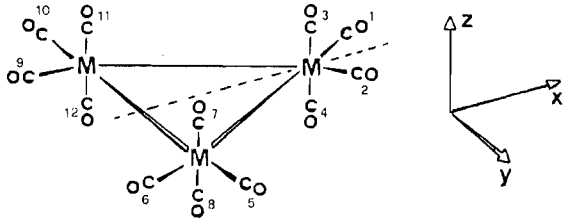

Figure 1. CO group labels and molecular axis choice used in Tables I and VII.

Table I. Convention Applied for the Numbering of the C–O Stretching Force Constants (K_i) and for the Direct (or Geminal, i_i) and Indirect (or Vicinal, j_i) Interaction Constants

$K_{eq} = f_1, f_2, f_5, f_6, f_9, f_{10}$
$K_{ax} = f_3, f_4, f_7, f_8, f_{11}, f_{12}$
i_1 (=i_{ee}) = $f_{1,2}, f_{5,6}, f_{9,10}$
i_2 (=i_{aa}) = $f_{3,4}, f_{7,8}, f_{11,12}$
i_3 (=i_{ea}) = $f_{1,3}, f_{1,4}, f_{2,3}, f_{2,4}, \cdots$
$j_1 = f_{1,10}, f_{2,5}, f_{6,9}$
$j_2 = f_{1,6}, f_{2,9}, f_{5,10}$
$j_3 = f_{1,5}, f_{1,9}, f_{2,6}, f_{2,10}, \cdots$
$j_4 = f_{3,7}, f_{3,11}, f_{4,8}, f_{4,12}, \cdots$
$j_5 = f_{3,8}, f_{3,12}, f_{4,7}, f_{4,11}, \cdots$
$j_6 = f_{1,11}, f_{1,12}, f_{2,7}, f_{2,8}, \cdots$
$j_7 = f_{1,7}, f_{1,8}, f_{2,11}, f_{2,12}, \cdots$

the two mixed compounds $Ru_2Os(CO)_{12}$ and $RuOs_2(CO)_{12}$, which were first reported by Lewis et al.,[18] but without spectroscopic data, and which were prepared in a spectroscopically pure state for this study.

Finally, we have made and report a detailed ν(CO) vibrational analysis in which C–O-factored force and interaction constants were calculated for both triosmium and triruthenium compounds by the use of a parametric rotational method.[4] Also, approximate force constant analyses of $Ru_2Os(CO)_{12}$ and $RuOs_2(CO)_{12}$ were carried out. Correlations are presented between the solution IR spectra and those obtained for crystalline samples. Similarly, the correlations between the solid-state IR and Raman spectra are given, the correlation including also the spectra of mixed crystals of the two homotrinuclear species.

The Molecular Problem

Throughout the present study we assume that the $M_3(CO)_{12}$ species (M = Ru, Os) have strict D_{3h} symmetry. Similarly, $Ru_nOs_{3-n}(CO)_{12}$ (n = 1, 2) species are assumed to have a C_{2v} structure derived immediately from the D_{3h}. In the latter symmetry it is convenient to first divide the stretching vibrations of the terminal CO groups into two sets, corresponding to those of the two sets of symmetry-related CO groups. The schematic structure of the $M_3(CO)_{12}$ molecules and the numbering scheme of the ligands are shown in Figure 1; the symbols used for the force and interaction constants are defined in Table I.

The vibrations of the CO groups which are coplanar with the metal triangle (the radial CO groups) give rise to normal vibrations of A_1' (R), A_2' (—), and 2 E′ (IR, R) symmetries, the spectral activities being given in parentheses (IR = infrared active; R = Raman active); the A_2' vibration is silent in harmonic vibrations. In contrast, the vibrations of the six out-of-plane (axial) groups transform as A_1' (R), A_2'' (IR), E′ (IR, R), and E″ (R), where, again, activities are indicated. Two problems are at once evident. First, mixing between axial and radial CO vibrations will occur for A_1' and E′ species affecting five of the seven spectrally active bands. Second,

(7) C. O. Quicksall and T. G. Spiro, *Inorg. Chem.*, **7**, 2365 (1968).
(8) D. Hartley, P. A. Kilty, and M. J. Ware, *Chem. Commun.*, 493 (1968).
(9) D. B. W. Yawney and F. G. A. Stone, *J. Chem. Soc. A*, 502 (1968).
(10) M. Poliakoff and J. J. Turner, *J. Chem. Soc. A*, 654 (1971).
(11) E. R. Corey and L. F. Dahl, *Inorg. Chem.*, **1**, 521 (1962).
(12) R. Mason and A. I. M. Rae, *J. Chem. Soc. A*, 778 (1968).
(13) (a) M. R. Churchill and B. G. DeBoer, *Inorg. Chem.*, **16**, 878 (1977); (b) M. R. Churchill, F. J. Hollander, and J. P. Hutchinson, *ibid.*, **16**, 1655 (1977).
(14) M. Arif and S. F. A. Kettle, *J. Chem. Phys.*, **72**, 2131 (1980).
(15) The low-frequency region is the subject of a separate paper.[16]
(16) S. F. A. Kettle and P. L. Stanghellini, *Inorg. Chem.*, **18**, 2749 (1979).
(17) Spectra obtained from mixed crystals show frequencies that vary smoothly with composition when intermolecular vibrational coupling occurs. Further, abnormal intensity changes occurring simultaneously are indicative of the presence of intensity stealing. A detailed study of such effects may enable one to comment on the molecular origins of the features appearing in the rather complicated spectra obtained in the ν(CO) region, thus providing a method which, in favorable cases, goes some way toward bridging the gap between molecular and crystal spectra. Other studies on mixed crystals of metal carbonyl species have recently been reported.[14]
(18) (a) B. F. G. Johnson, R. D. Johnson, J. Lewis, I. G. Williams, and P. A. Kilty, *Chem. Commun.*, 861 (1968); (b) G. L. Geoffrey and W. L. Gladfelder, *J. Am. Chem. Soc.*, **99**, 304 (1977); (c) R. P. Ferrari, G. A. Vaglio, and M. Valle, *J. Chem. Soc., Dalton Trans.*, 1164 (1978).

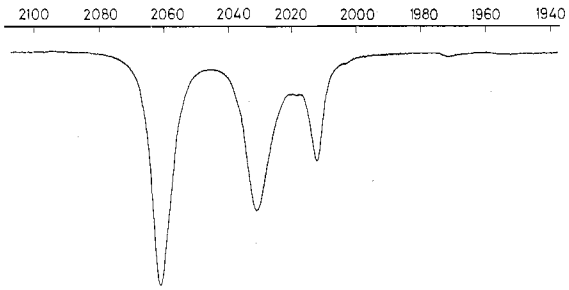

Figure 2. Infrared spectrum of $Ru_3(CO)_{12}$ in the 2000-cm^{-1} region (hexane solution).

in the solid phase, in the presence of general intramolecular vibrational coupling, the space group symmetry of $P2_1/n$ (C_{2h}^5) will enforce an exclusion between the infrared- and the Raman-active factor group components which arise from a molecular mode which is both infrared and Raman active. The difficulties of obtaining an unambiguous interpretation of infrared and Raman spectra obtained from crystalline samples are evident, even if the consequences of the (strict) molecular C_1 symmetry in the crystal lattice are neglected. In the case of the Os_2Ru and $OsRu_2$ species the idealized molecular symmetry drops to C_{2v} so that all degeneracies are relieved at the molecular level.

For an isolated, D_{3h} $M_3(CO)_{12}$ molecule there are four ν(CO) modes which should be infrared active, of symmetry species 1 A_2'' + 3 E'.

The two assignments of these bands in the literature are in conflict in that Kaesz et al.[6] assigned the purely axial A_2'' mode to the second highest band (observed for $Os_3(CO)_{12}$ at 2035 cm^{-1} by these authors), whereas Quicksall and Spiro[7] assigned the highest energy IR band (observed by these authors at 2062 and 2070 cm^{-1} for $Ru_3(CO)_{12}$ and $Os_3(CO)_{12}$, respectively) to this vibration.

Moreover, Kaesz et al. suggested that the frequency order of the three E' modes is e'(axial) > e'(radial, a_1) > e'(radial, b_1). Here "axial" and "radial" refer obviously to that symmetry coordinate which dominates in the vibration and the symmetry descriptors a_1 and b_1 of the radial (equatorial) modes refer to their local symmetry approach where an $Os(CO)_4$ entity of local C_{2v} symmetry is considered.

As we have indicated, Quicksall and Spiro[7] based their assignment on the application of IR and Raman selection rules appropriate to the free molecule to spectra on solid samples. They stated that "since the basic features of the spectrum with one exception could be explained without invoking crystal effects, these will not be considered further". Unfortunately, no ν(CO) spectra were shown graphically in their paper. However, our results reproducibly and consistently showed strong crystal effects (vide infra). Hence we suppose that inefficient spectral resolution was the reason for the lack of observing such effects by these authors. Their criteria of assignment cannot, therefore, be accepted.

In our study we have systematically varied the possible assignments of the IR bands and reached the conclusion that the assignment proposed by Kaesz et al.[6] for the IR-active modes is correct: this was the only one to yield relative magnitudes of "through-metal-atom" (i.e., geminal, or direct) and through M–M bond (i.e., vicinal, or indirect) CO···C'O' interaction constants, similar to those obtained earlier for a variety of di-, tri-, and tetranuclear carbonyls.[2-4,19,20] It is to be emphasized that although the present work has confirmed this assignment, this statement applies only to the assignment

(19) G. Bor and G. Sbrignadello, *J. Chem. Soc., Dalton Trans.*, 440 (1974).
(20) G. Sbrignadello, G. Battiston, and G. Bor, *Inorg. Chim. Acta*, **14**, 69 (1975).

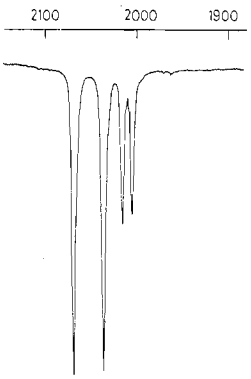

Figure 3. Infrared spectrum of $Os_3(CO)_{12}$ in the 2000-cm^{-1} region (hexane solution).

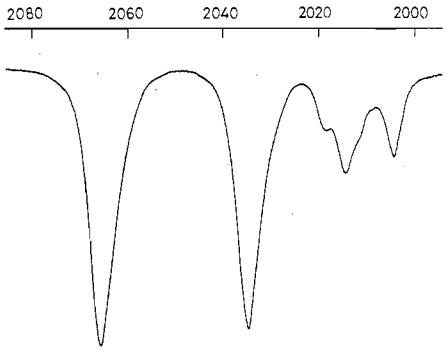

Figure 4. Infrared spectrum of $Ru_2Os(CO)_{12}$ in the 2000-cm^{-1} region (hexane solution).

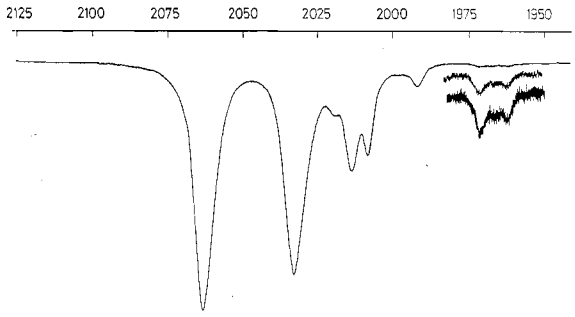

Figure 5. Infrared spectrum of $RuOs_2(CO)_{12}$ in the 2000-cm^{-1} region (hexane solution).

Table II. Correlation between Symmetry Species of Point Groups D_{3h} and C_{2v}

D_{3h}	A_1'	A_1''[a]	A_2'	A_2''	E'	E''
C_{2v}	A_1	A_2	B_1	B_2	$A_1 + B_1$	$A_2 + B_2$[b]

[a] No C-O stretching modes belonging to this species occur. [b] Concerning the notation of symmetry species B_1 and B_2 for $M'M_2(CO)_{12}$, we adopt the convention that z is taken as the two-fold axis and the y axis is perpendicular to the $M'M_2$ plane.

of the local symmetry coordinates. Kaesz et al.[6] did not deal with, for instance, the extent of coupling between the three sets of symmetry coordinates of symmetry species E' or with the assignment of the IR-inactive modes.

The Quicksall–Spiro assignment does not permit agreement to be obtained between calculated and observed ^{13}CO frequencies; in addition, it results in improbable interaction force constant values.

Results and Discussions

1. Assignments. In agreement with D_{3h} symmetry, four bands are observed in the relevant region of the solution infrared spectra of $Ru_3(CO)_{12}$ (Figure 2) and $Os_3(CO)_{12}$ (Figure

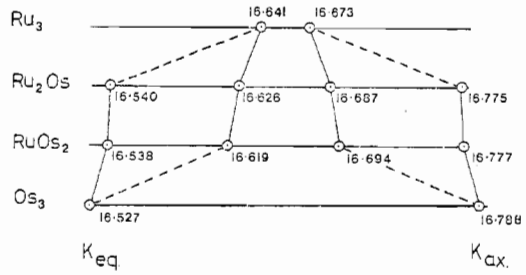

Figure 6. Correlation between CO bond stretching force constants in Ru_3-, Ru_2Os-, $RuOs_2$-, and $Os_3(CO)_{12}$.

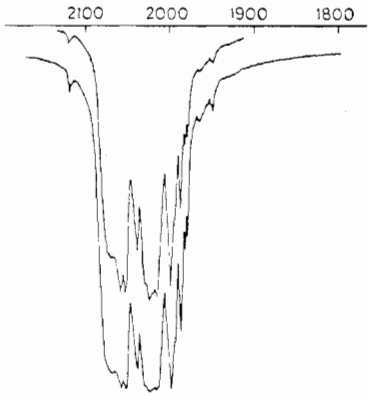

Figure 7. ν(CO) infrared spectra of polycrystalline $Ru_3(CO)_{12}$ (KBr disk, two concentrations).

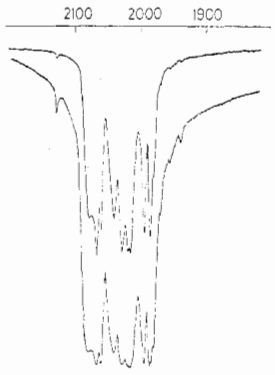

Figure 8. ν(CO) infrared spectra of polycrystalline $Os_3(CO)_{12}$ (KBr disk, two concentrations).

Figure 9. ν(CO) infrared spectra of polycrystalline $Ru_2Os(CO)_{12}$ (KBr disk, two concentrations).

3), although for the former one of these bands is of quite low intensity (vide infra).

The solution infrared spectra of the species $Ru_2Os(CO)_{12}$ and $RuOs_2(CO)_{12}$ are shown in Figures 4 and 5, respectively.

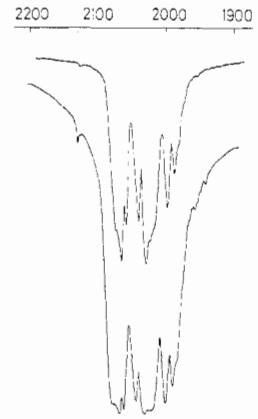

Figure 10. ν(CO) infrared spectra of polycrystalline $RuOs_2(CO)_{12}$ (KBr disk, two concentrations).

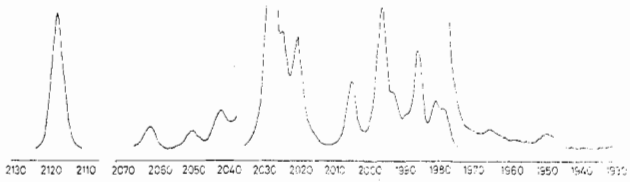

Figure 11. ν(CO) Raman spectra of polycrystalline $Ru_3(CO)_{12}$. The ca. 2050-cm^{-1} and ca. 1950-cm^{-1} regions are shown at a higher sensitivity.

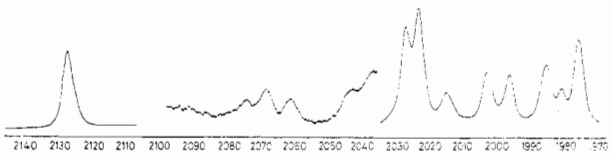

Figure 12. ν(CO) Raman spectra of polycrystalline $Os_3(CO)_{12}$. The ca. 2070-cm^{-1} region is shown at a higher sensitivity.

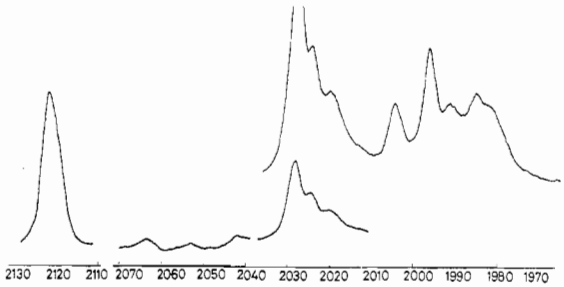

Figure 13. ν(CO) Raman spectra of polycrystalline $Ru_2Os(CO)_{12}$. The ca. 2050-cm^{-1} region is shown at a higher sensitivity.

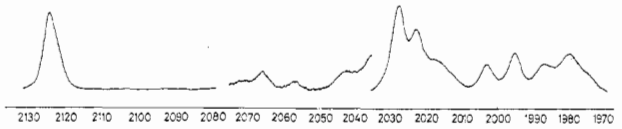

Figure 14. ν(CO) Raman spectra of polycrystalline $RuOs_2(CO)_{12}$. The ca. 2060-cm^{-1} region is shown at a higher sensitivity.

The correlation between D_{3h} and C_{2v} symmetry which we adopt is shown in Table II. In examining the data given in Figures 2–5, it is helpful to anticipate to some extent our final conclusions. In Figure 6 we show the correlations between the axial and radial CO stretching force constants of the four species. It is clear that these constants exhibit a nearly perfect transferability from molecule to molecule. Not surprisingly, this transferability has strong spectral implications.

In Figures 7–10 are shown the solid-state infrared spectra corresponding to those of Figures 2–5 while the corresponding

Table III. Solid-Phase IR and Raman Frequencies (±1–2 cm^{-1})

$Ru_3(CO)_{12}$		$Ru_2Os(CO)_{12}$		$RuOs_2(CO)_{12}$		$Os_3(CO)_{12}$	
IR	Raman	IR	Raman	IR	Raman	IR	Raman
2120.5 vw	2119 s	2123 vw	2121.5 s	2126 vw	2124 s	2129 vw	2127 s
ca. 2071 m, br		ca. 2073 s, br		ca. 2072 s, br		ca. 2080[a] m, br	2075 vw
2060 s	2062.5 vw	2062 s	2064 vw	2066 s	2065 vw	2068 s	2068 vw
2054 s	2050 vw	2056 s	2053 vw	2058.5 s	2056 vw	2061 s	2061 vw
2040 m	2042 vw	2040 m	2042 vw	2041 s	2042 vw	2041 m	ca. 2042 vw
2032 m	2028 vs						
2027 s	2024.5 m	2028 s	2028.5 s	2030 s	2027.5 s	2029 s	2026 s
			2024.5 m		2023 m		
2022 s	2020.5 m	ca. 2021 s, br	2020 w	ca. 2018–2022[b] m, br	ca. 2018 m, sh	2020 s	2022 s
2017 s						2016 s	2014 w
	2005 m		2004.5 m		2003.5 m		2002 m
1999 s		1999 s		1998 s		1996 s	
	1996.5 s		1996.5 m		1995.5 m		1995.5 m
1995 m, sh		1992 w					
	1993 w		1991 w				
1988 m	ca. 1989 vw, sh	1988 m	1985 m	1988 m	1987.5 m	1986 s	1984.5 m
	1986 m					1984 m, sh	
1982 w	1981 w						
1979 w	1978.5 w	ca. 1982 w, sh	ca. 1983 w, sh	ca. 1981 w, sh	1980.5 m	1980 m	1980 w
ca. 1965 vw	1965.5 vw	ca. 1971 vw, sh		ca. 1973 vw, sh	ca. 1976 w, sh	1970 w	1975 s
1956 vvw		1961 vvw		1955 vvw	ca. 1953 vw	1956 vw	
		1956 vvw				1952 vvw	
ca. 1949 vw	1949.5 vw	1950 vvw		ca. 1948 vvw, sh		1948 vvw	
		ca. 1940 vvw		1939 vw		1940 vw	ca. 1941 vw

[a] Shifts in repeatedly ground and repressed pellets from ca. 2084 to ca. 2078 cm^{-1}. [b] Probably doublet.

Table IV. Comparison of the Calculated and Observed (Hexane Solution) Spectra (cm^{-1}) of the $M_3(^{12}CO)_{11}(^{13}CO)$ Equatorial (eq) and Axial (ax) Isomers with the C–O Stretching Frequencies of the Parent $M_3(CO)_{12}$ Compounds

		$Ru_3(^{12}CO)_{11}(^{13}CO)$					$Os_3(^{12}CO)_{11}(^{13}CO)$		
		calcd					calcd		
assignt	$Ru_3(CO)_{12}$	eq	ax	obsd	assignt	$Os_3(CO)_{12}$	eq	ax	obsd
$\nu_1(A_1')$	2120.0	2117.4	2117.1	2116.0	$\nu_1(A_1')$	2130.0	2128.1	2126.2	
$\nu_5(E')$	2061.2	2061.1	2061.2		$\nu_5(E')$	2069.0	2068.9	2069.0	
		2057.4	2056.4	2057.4			2065.7	2062.7	2064.0
$\nu_2(A_1')$	2036.0	2034.1	2034.9	2035.0	$\nu_2(A_1')$	2038.0	2035.3	2037.6	2033.5
$\nu_4(A_2'')$	2031.3	2031.3	2026.5	2027.5	$\nu_4(A_2'')$	2036.5	2036.5	2029.9	2030.0
$\nu_6(E')$	2018.7	2018.7	2018.7		$\nu_6(E')$	2015.6	2015.6	2015.6	
		2016.6	2014.1	2013.5			2012.2	2011.5	2012.1
$\nu_7(E')$	2012.5	2012.5	2012.5		$\nu_7(E')$	2004.7	2004.7	2004.7	~2003 (?)
		2004.1	2010.9	2004.0			1993.9	2004.7	1994.0
$\nu_3(A_2')$	1999.5	1972.0	1999.5[a]	1972.0	$\nu_8(E'')$	1995.0	1995.0[a]	1995.0[a]	
$\nu_8(E'')$	1994.5	1994.5[a]	1994.5[a]				1995.0[a]	1969.6	1969.5
		1994.5[a]	1968.0	1968.0	$\nu_3(A_2')$	1987.0	1962.8	1987.0[a]	1962.5

[a] Calculated intensity = 0.

Raman spectra are shown in Figures 11–14. Frequency data for polycrystalline samples are collected in Table III.

The solution IR spectra of ^{13}CO-enriched $Ru_3(CO)_{12}$ are shown in Figure 15; and all isotopic data are detailed in Table IV.

In all of these spectra there is never any doubt as to the assignment of the highest C–O mode: this is the totally symmetric mode (A_1' or A_1), with an in-phase coupling of the axial and radial vibrators. We find that the extent of coupling is quite strong for all of the compounds studied. This vibration is IR inactive according to ideal (isolated) D_{3h} selection rules but shows a slight intensity in the solid-phase IR spectra. This could be due to a lattice-induced distortion of the molecule. In C_{2v} symmetry this vibration is formally IR active, but it exhibits an intensity similar to that of the D_{3h} species.

Because the very low solubility of these compounds inhibited the observation of the Raman spectra in solution and the solid-state Raman spectra are not directly applicable for exact frequency assignments, the main sources of exact data from which to determine the frequencies of the IR-inactive modes were the ^{13}CO satellites. In the case of the highest energy (A_1' or A_1) mode the IR spectra of KBr pellets of the solids gave

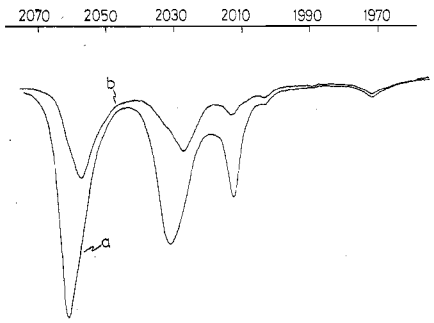

Figure 15. The infrared spectra of ca. 5% ^{13}CO-enriched $Ru_3(CO)_{12}$ in the 2000-cm^{-1} region (hexane solution): (a) uncompensated spectrum; (b) a spectrum in which the absorption due to the all-^{12}CO species has been almost completely compensated.

frequencies which agreed very well (within ±1 cm^{-1}) with the frequencies calculated from the (very weak) ^{13}CO satellites measured in solution and with the frequencies obtained from the solid-phase Raman spectra. It seems to be frequently the case that pseudospherically symmetric ν(C–O) normal modes

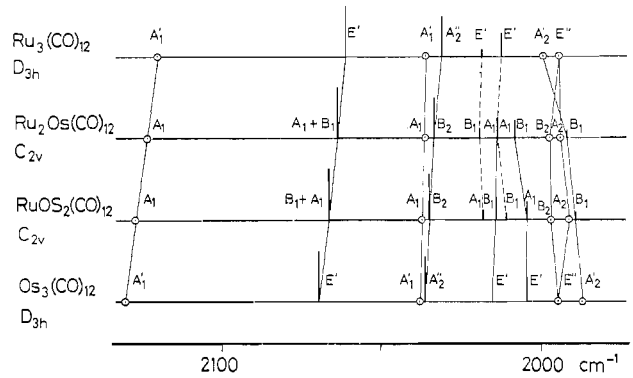

Figure 16. Correlation between ν(CO) stretching frequencies of Ru_3-, Ru_2Os-, $RuOs_2$-, and $Os_3(CO)_{12}$. Vertical bars indicate the relative intensities of infrared-active modes. Solution frequency data are given for the active modes; other frequencies are calculated from ^{13}CO-containing species. Full filiation lines indicate an unambiguous parentage, and dotted lines indicate major parentage. No filiation lines are given for species of mixed parentage.

suffer at most a very small frequency shift and/or broadening when going from the dissolved to the solid state.

The second highest features in the spectra of the four complexes are (i) in the solution IR spectra a strong band in the range 2070–2060 cm^{-1}, (ii) in the solid IR spectra three bands for each complex in the 2075–2054-cm^{-1} region, and (iii) in the solid Raman spectra two weak bands (but three for $Os_3(CO)_{12}$) in the 2075–2050-cm^{-1} region.

It seems clear that these features all have the same molecular origin. It surely belongs to an IR-active species. Either it is Raman forbidden and yet gained some intensity or it is Raman active but for some reason very weak. The first case corresponds to a species of symmetry A_2'', in agreement with the suggestion of Quicksall and Spiro; the second case would imply an assignment as E′ (axially dominated), corresponding to the proposal of Huggins, Flitcroft, and Kaesz. As it has been pointed out above, the isotopic ^{13}CO satellites of these bands measured at 2064, 2063, 2059, and 2057.4 cm^{-1} for Os_3-, $RuOs_2$-, Ru_2Os-, and $Ru_3(CO)_{12}$, respectively, fit the calculations very well only when assigned as E′, and only this assignment yielded interaction constants in line with previous results.

Further support for this assignment comes from intensity arguments. In the highest frequency E′-type vibration (where the relative contribution of the equatorial and axial vibrators is ax > eq) there is surely a very high intensity contribution from an "induced dipole moment"[3,4,21] (or "orbital following"[2c] or "vibronic"[22]) mechanism, which adds to the intensity due to the local C–O dipoles.

In the triad Mn–Tc–Re (where this intensity enhancement mechanism is reflected by the higher B_2 mode of D_{4d} symmetry) this effect decreases with increasing atomic mass of the metals.[23] For these trinuclear complexes, the band which would be expected to show this effect is of E′ type in D_{3h} symmetry; the effect (relative to the second strong IR band) is observed for the band under discussion. This E′ mode gives rise to two species (A_1 and B_1), both IR and Raman active, in C_{2v} symmetry for the mixed complexes in solution. The correlation between E′ and A_1/B_1 modes, shown in Figure 16, is very good. The computations carried out on the mixed complexes suggest that the species A_1 and B_1 are little separated in frequency (less than 1 cm^{-1}) and give rise to only one band, with an intensity equal to the sum of the relative intensities. If the splitting were significant, it should be visible in the spectra, owing to the medium calculated intensity of each component.

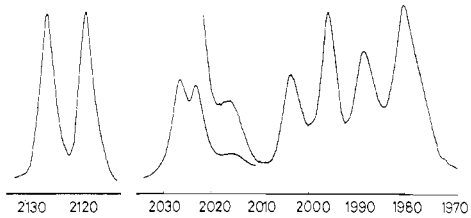

Figure 17. ν(CO) Raman spectrum of a polycrystalline mixed crystal containing $Ru_3(CO)_{12}$ and $Os_3(CO)_{12}$ in an approximately 1:1 ratio.

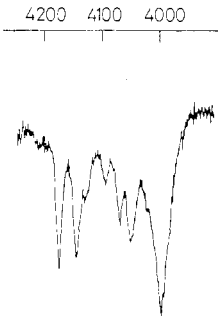

Figure 18. Infrared spectrum of $Ru_3(CO)_{12}$ in the ν(CO) combination/overtone region (CCl_4 solution).

It is reasonable that the Raman intensity of this E′ mode should be low. If the derived polarizability tensor at each axial CO group is cylindrically symmetrical about an axis parallel to the threefold axis, then a simple Wolkenstein model predicts a zero contribution to the intensity. There is no symmetry requirement for cylindrical symmetry, and so some small axial CO-derived $d\alpha(CO)_\perp/dr$ intensity is expected. This must be added to the contribution from the radial CO's, a contribution which comes from $d\alpha(CO)_\parallel/dr$. Frequently, $d\alpha(CO)_\perp/dr$ and $d\alpha(CO)_\parallel/dr$ are of opposite sign for metal carbonyls, and so axial and radial contributions to the intensity will tend to cancel. In the IR and Raman solid spectra there is splitting of this E′ band possibly caused by site symmetry and correlation field effects. However, some other phenomenon may also be present because the broad bands in the 2070–2060-cm^{-1} region are sensitive to the extent of grinding of the samples.

The solid-state Raman spectra are helpful in assigning A_1' modes. Two strong A_1' peaks are expected at high frequencies because both involve in-phase vibrations of symmetry-related CO groups; they will almost certainly be two mode in nature (that is, show no factor group splitting and appear as separate Ru and Os features in mixed crystals) because of the high order of symmetric multipole interaction required to couple adjacent molecular vibrations in the crystal lattice. In accord with this expectation, the highest frequency peaks in the Ru_3 and Os_3 spectra are clearly two mode, as expected for an A_1' mode-derived feature. This may be seen in Figure 17 which shows the Raman spectra of ca. 1:1 mixture of the two homo species crystallized together.

We similarly believe that the peak seen at ca. 2032 cm^{-1} corresponds to the second A_1'-derived feature. Its position varies by only 2.5 cm^{-1} between the pure osmium and ruthenium spectra, so, notwithstanding our belief that this feature exhibits two-mode behavior, we would not expect to see two peaks in Figure 17 (our Raman slit width was generally 2 cm^{-1}). In support for our belief of two-mode behavior we note that this feature shows no intensity change throughout the entire range of mixed-crystal spectra, a behavior compatible only with either limiting two- or one-mode behavior. Were it to exhibit one-mode behavior, we would expect similar be-

(21) F. A. Cotton and R. M. Wing, *Inorg. Chem.*, **4**, 1328 (1965).
(22) D. J. Darensbourg and T. L. Brown, *Inorg. Chem.*, **7**, 959 (1968).
(23) G. Battiston, Thesis, University of Padua, 1971–1972.

Table V. Assignment of the Observed (CCl_4 Solution) and Calculated C-O Stretching Combination and Overtone Bands (cm^{-1}) of $Ru_3(CO)_{12}$

obsd	calcd	assignt
4175	4181	$\nu_1 + \nu_5(E')$
4146	4151	$\nu_1 + \nu_4(A_2'')$
4128 sh[a]	4132	$\nu_1 + \nu_7(E')$
4095	4097	$\nu_2 + \nu_5(E')$
4069	4067	$\nu_2 + \nu_4(A_2'')$
4049	4049	$\nu_2 + \nu_7(E')$
4020 sh[a]	4026	$\nu_4 + \nu_8(E')$
	4025	$2\nu_7(E')$
3996	4007	$\nu_7 + \nu_8(A_2'')$

[a] sh = shoulder.

havior from adjacent factor group components. This is not observed.

Our interpretation of the combination spectra in the 4000-cm^{-1} region (Figure 18 and Table V) indicated that the second A_1' feature has a frequency of ca. 2035 cm^{-1} (for $Ru_3(CO)_{12}$) since only an $A_1' + E'$ combination can account for the bands observed at 4095, 4069, and 4049 cm^{-1}; it was the solution infrared spectrum of ^{13}CO-enriched $Ru_3(CO)_{12}$ which yielded the exact value: the weak band at ca. 2035 cm^{-1} in the spectrum of the slightly enriched sample (^{13}CO content ca. 5%) scanned with varying compensation of the all-^{12}CO bands can have no other origin than the derivatives of the $\nu_2(A_1')$ mode. The value of 2036 cm^{-1} was calculated as the $\nu_2(A_1')$ frequency for all-^{12}CO $Ru_3(CO)_{12}$, which upon mono-^{13}CO substitution in the axial position gives rise to an IR-active mode at 2035 cm^{-1}.

The analogous approach was not successful in the case of $Os_3(CO)_{12}$. First, the spectrum of the ^{13}CO-enriched sample did not show a feature around 2036–2038 cm^{-1} where the bands of the mono-^{13}CO molecules were to be expected; the closeness of the very strong A_2'' mode made observation of any weak peak impossible even in the spectra where the all-^{12}CO bands had been compensated. Second, the very low solubility of $Os_3(CO)_{12}$ did not enable the observation of the combination spectrum around 4000 cm^{-1}. Hence the good linearities generally observed in the correlations of corresponding symmetry species through $Ru_3(CO)_{12}$, $Ru_2Os(CO)_{12}$, $RuOs_2(CO)_{12}$, and $Os_3(CO)_{12}$ encouraged us to tentatively extrapolate in a consistent way to obtain the corresponding frequencies of osmium-containing species. The good correlations found with the Raman and solid-state IR spectra confirmed the validity of this approach.

A very strong feature is observed in the solid IR spectra at 2041, 2041, 2040, and 2040 cm^{-1} for Os_3-, $RuOs_2$-, Ru_2Os-, and $Ru_3(CO)_{12}$, respectively. This absorption is associated with strong bands at 2036.5, 2035.2, 2033.5, and 2031.3 cm^{-1}, respectively, in the solution IR spectra, and it has a Raman counterpart in the band at 2042 cm^{-1} (for all complexes) with a weak intensity. We assign these frequencies to A_2'' (D_{3h}), IR only active (B_2 in C_{2v}). These modes are expected to be the strongest IR bands in the solution spectra (if one neglects the induced dipole contribution), and after the assignment of the highest energy IR band (2070–2060 cm^{-1}) to an E′ mode, there are no other candidates for this vibration, ν_4. This assignment agrees with that of Huggins, Flitcroft, and Kaesz; the correlation of this mode through the various molecular species is quite unambiguous. The weak crystal Raman feature for this mode, Raman forbidden in D_{3h}, can be explained by the low crystal site symmetry.

A particularly interesting aspect of this assignment concerns the solution–crystal correlation. It may be remarked that for metal carbonyls a regularity seems to hold in that the solid-phase frequencies are usually lower than those obtained in solution spectra. Further, this solid-state effect is stronger the lower the frequency in a given spectrum. Thus, the totally symmetric vibrations above 2100 cm^{-1} usually show no shifts or only very small ones, whereas the frequencies below 2000 cm^{-1} are usually strongly shifted in the solid-state spectra. This generalization does not hold for the A_2'' bands of these compounds. Discounting experimental frequency uncertainties, which we have taken care to remove in the present work, the most probable explanation is that correlation field effects occur and cause an apparent high-frequency shift. The high dipolar activity of the A_2'' mode leads to an expectation of strong intermolecular vibrational coupling for this mode; if the infrared activity is largely concentrated in one factor group component and this component is at relatively high frequency, then the observed frequency shift is explained.

Two E′ (or derived symmetry) modes are assigned to the region between 2020 and 2000 cm^{-1} in all of the compounds. In the solution infrared spectrum these bands are only of moderate or weak intensity; the solid-state infrared spectra are more complex but correlate well with the solid-state Raman spectra, where the intensity is higher. It is clear in the latter that some intensity stealing may occur because a consistent intensity pattern is not observed. However, the two bands in the 2010–2000-cm^{-1} region appear to be members of a degenerate pair split by static field effects. Thus, in the Os_3 complex these bands have almost identical intensities and are relatively remote from other features which, for the other compounds in the series, appear to both move closer and transfer intensity. There is a clear correlation of these features through the mixed-crystal spectra with those of the pure ruthenium compound. In the latter, the intensity pattern is different, although this may well be a consequence of the greater factor group splitting of the low-frequency peaks leading to a superposition of features. We have no evidence for anything other than two-mode behavior for the E′-derived peaks.

We have found, as a result of the final refinement of our analysis after the assignment of all C–O stretching modes, that there is a very strong mixing between the E′(ax) and E′(radial, a_1) modes, whereas the E′(radial, b_1) mode is relatively pure. This mixing of the E′ symmetry coordinates will most probably be sensitive to site symmetry effects and may well account for the intensity changes seen in our Raman spectra. Certainly, these are entirely consistent with the presence of two E′ modes both split and mixed by static field effects.

The normal coordinate calculations also revealed a somewhat complicated situation. Huggins, Flitcroft, and Kaesz assigned the frequencies at 2015.6 and 2004.7 cm^{-1} to E′ modes (radial A_1 and B_1, respectively) on the local symmetry basis. We agree with this assignment since also in our approach we note that the two E′ modes are dominantly radial in character. However, in the mixed complexes both E′ modes in this region are split even in the solution IR spectra (four bands or shoulders observed for $RuOs_2(CO)_{12}$ and three for $Ru_2Os(CO)_{12}$). In excellent agreement with these observations the computations showed that the splitting of the components should be of the order of 4–7 cm^{-1} (an overlap between the lower component of the higher E′ mode and the higher component of the lower E′ mode is responsible for the fact that only three bands are observed for Ru_2Os and that the middle one is of much higher intensity). The analysis of the eigenvectors of these vibrational modes shows that the sequence of the symmetry species for the split components is inverted in going from Ru_2Os to $RuOs_2$. This originates in the different values of the homonuclear stretching force constants. To explain this, let us define as M_x the metal atom which becomes unique in the mixed species (since the x axis passes through the center of the M_3 triangle and M_x). Then, in other words, the eigenvectors of the x components of the higher E′ mode

(local a_1) for both Os_3 and Ru_3 represent vibrations mainly localized at M_x while the orthogonal components (y) are mainly localized at the other metal atoms. In contrast to this in the *lower* E′ mode of Os_3 and Ru_3 (local b_1) the vibration mainly localized at M_x is the y component, and the other two metal atoms are involved in the x component. In the case of the mixed compounds for both E′ modes the x components become A_1 and the y components B_1. Since $K_{eq}(Ru_3) > K_{eq}(Os_3)$, in the $RuOs_2$ case the sequence of the assignment is $A_1B_1B_1A_1$, while in the Ru_2Os case it is $B_1A_1A_1B_1$. Throughout the series (i.e., Ru_3-, Ru_2Os-, $RuOs_2$-, $Os_3(CO)_{12}$), there is a consistent pattern in that the local symmetry of the vibration of the $M(CO)_4$ units is always a_1 for the higher pair of vibrations and that for the lower pair is always b_1.

The low-frequency ^{13}CO satellites at 1972 and ca. 1968 cm^{-1} (shoulder) in the solution infrared spectrum of $Ru_3(CO)_{12}$ and the corresponding bands of $Os_3(CO)_{12}$ at ca. 1969 and 1962 cm^{-1} indicated the presence of *two* all-^{12}CO frequencies in the region between 2000 and 1990 cm^{-1} (for these complexes). Only the A_2' and E″ modes were realistic candidates for this region. Quicksall and Spiro assigned the lowest of all the C–O frequencies to the (IR and Raman inactive) A_2' mode; this vibration is an in-phase coupling of local b_1-type vibrations. All observations but one were compatible with this assignment: for $Ru_3(CO)_{12}$ the mono-^{13}CO band at 2004 cm^{-1} cannot be fitted with any combinations of the parameters when E″ > A_2'. When this order was reversed, an excellent fit between observed and calculated mono-^{13}CO frequencies was achieved.

There are several points to be noted in connection with this assignment. First, the monomeric species $Ru(CO)_5$ has a strong band at 2004 cm^{-1} and may be formed photochemically even under 1 atm of CO.[24] Accordingly, it was necessary to ascertain that this species was not present as an impurity. Its absence was established in two different ways after the exchange reaction with ^{13}CO had been carried out in darkness; the enriched sample was kept for a long period under high vacuum to eliminate any of the more volatile $Ru(CO)_5$ formed, the enriched sample was chromotographed on a silica-gel column, and several fractions were checked spectroscopically. In each case no change of relative band intensities before and after the treatment could be observed. Hence the authenticity of the 2004-cm^{-1} band in the ^{13}CO-enriched spectrum of $Ru_3(CO)_{12}$ is assured.

Second, since the A_2'-type vibration (→B_1 in the mixed complexes) is a purely radial mode, it is in accord with the increase (Figure 6) of K_{eq} in the series $Os_3 < RuOs_2 < Ru_2Os < Ru_3$ that the frequency of this vibration increases correspondingly. Similarly, the E″ mode (and the $B_2 + A_2$ modes derived from it in the $M_2M'(CO)_{12}$ cases) is purely axial; hence the decrease of K_{ax} in the same series requires the decrease of these frequencies. The trend found in the assignment of these modes, which requires a crossing of the filiation lines between Ru_2Os- and $Ru_3(CO)_{12}$ (Figure 16), is therefore completely consistent. It should be noted that the direct connection between the E″ and A_2' modes and the low isotopic satellites which derive mainly from them ensured that the frequencies of these two IR-inactive modes could be determined with accuracy.

Third, we note that the A_2' modes of the D_{3h} molecules gain some intensity when they become B_1 in C_{2v}. The pseudorotation character of this vibration is retained, however, with somewhat different amplitudes of the local b_1 vibrations of the radial ligands, so that a slight dipole moment change occurs during the vibration.

Fourth, the A_2 component of the split E″ mode in the mixed complexes remains strictly IR inactive in overall C_{2v} symmetry.

(24) B. F. G. Johnson, J. Lewis, and M. V. Twigg, *J. Organomet. Chem.*, **67**, C75 (1974).

Table VI. Frequencies (cm^{-1}) and Assignments of the C–O Stretching Fundamentals of $Ru_3(CO)_{12}$, $Ru_2Os(CO)_{12}$, $RuOs_2(CO)_{12}$, and $Os_3(CO)_{12}$, in Hexane Solution

$Ru_3(CO)_{12}$	$Ru_2Os(CO)_{12}$	$RuOs_2(CO)_{12}$	$Os_3(CO)_{12}$
2120.0[e] a_1'	*2123.0* a_1	*2126.9* a_1	*2130.0* a_1'
2061.2 e′	2063.7[a] a_1	2066.4[b] b_1	2069.0 e′
	2063.6[a] b_1	2066.3[b] a_1	
2036.0 a_1'	*2036.5* a_1	*2037.5* a_1	*2038.0* a_1'
2031.3 a_2''	2033.5 b_2	2035.2 b_2	2036.5 a_2''
2018.7 e′	2019.5 b_1	2018.7 a_1	2015.6 e′
	2014.0[c] a_1	2014.7 b_1	
2012.5 e′	2013.9[c] a_1	2011.2 b_1	2004.7 e′
	2008.7 b_1	2004.7 a_1	
1994.5 e″	1997.5[d] b_2	1997.0[d] b_2	*1995.0* e″
	1994.0 a_2	*1991.5* a_2	
1999.5 a_2'	1992.2 b_1	1989.7 b_1	*1987.0* a_2'

[a] Calculated values; observed at 2063.7 cm^{-1}. [b] Calculated values; observed at 2066.4 cm^{-1}. [c] Calculated values; observed as a single band at 2014.0 cm^{-1}. [d] Very, very weak bands; observed only with ordinate expansion (cf. text). [e] N.B. Values in *italics* cannot be observed directly in solution IR spectra. These were calculated as explained in the text.

Table VII. Form of C–O Stretching Symmetry Coordinates Adopted in This Study

$$S_1(A_1') = (\Delta r_1 + \Delta r_2 + \Delta r_5 + \Delta r_6 + \Delta r_9 + \Delta r_{10})/6^{1/2}$$
$$S_2(A_1') = (\Delta r_3 + \Delta r_4 + \Delta r_7 + \Delta r_8 + \Delta r_{11} + \Delta r_{12})/6^{1/2}$$
$$S_3(A_2') = (\Delta r_1 - \Delta r_2 + \Delta r_5 - \Delta r_6 + \Delta r_9 - \Delta r_{10})/6^{1/2}$$
$$S_4(A_2'') = (\Delta r_3 - \Delta r_4 + \Delta r_7 - \Delta r_8 + \Delta r_{11} - \Delta r_{12})/6^{1/2}$$
$$S_{5x}(E') = (2\Delta r_3 + 2\Delta r_4 - \Delta r_7 - \Delta r_8 - \Delta r_{11} - \Delta r_{12})/12^{1/2}$$
$$S_{5y}(E') = (\Delta r_7 + \Delta r_8 - \Delta r_{11} - \Delta r_{12})/2$$
$$S_{6x}(E') = (2\Delta r_1 + 2\Delta r_2 - \Delta r_5 - \Delta r_6 - \Delta r_9 - \Delta r_{10})/12^{1/2}$$
$$S_{6y}(E') = (\Delta r_5 + \Delta r_6 - \Delta r_9 - \Delta r_{10})/2$$
$$S_{7x}(E') = (\Delta r_5 - \Delta r_6 - \Delta r_9 + \Delta r_{10})/2$$
$$S_{7y}(E') = (-2\Delta r_1 + 2\Delta r_2 + \Delta r_5 - \Delta r_6 + \Delta r_9 - \Delta r_{10})/12^{1/2}$$
$$S_{8x}(E'') = (2\Delta r_3 - 2\Delta r_4 - \Delta r_7 + \Delta r_8 - \Delta r_{11} + \Delta r_{12})/12^{1/2}$$
$$S_{8y}(E'') = (\Delta r_7 - \Delta r_8 - \Delta r_{11} + \Delta r_{12})/2$$

The other E″ derivative, B_2, may have, according to our calculations, a very slight IR intensity, depending on the weight of the (axial) vibrations at M_x, compared with that at the other two metal atoms. It was only a posteriori that we noticed an extremely weak absorption at the calculated position (1997 cm^{-1}) in solution spectra of both mixed compounds.

Finally, the intensity found in the bands in the below 2000-cm^{-1} region of the Raman spectra is surprising. Although the E″ mode is Raman allowed, arguments based on a Wolkenstein model suggest that its intensity should be low. However, not only is the intensity reasonably high but it is clear from the mixed-crystal spectra that intermolecular vibrational coupling occurs. The spectra show evidence of intermediate coupling, and it seems increasingly clear that such coupling is attended by intensity enhancement. In some simple systems it has been possible to establish that this is LO–TO and LA–TA in origin.[25]

The final assignment of all C–O stretching fundamentals is shown in Table VI.

2. C–O Stretching Force Constants and Normal Coordinates. The numbering and construction of the symmetry coordinates applied in this study are given in Table VII. The force and interaction constants obtained within the framework of an energy factored model are compiled in Table VIII. The symbols used for the force and interaction constants are explained in Table I. A graphical representation of the "filiation lines" of the C–O stretching valence force constants is given

(25) See, for example: (a) R. J. Elliott, W. Hayes, G. D. Jones, H. F. Macdonald, and C. T. Sennett, *Proc. R. Soc. London, Ser. A*, **289**, 1 (1965); (b) C. A. Arguello, D. L. Rousseau, and S. P. S. Porto, *Phys. Rev.*, **181**, 1351 (1969); (c) C. M. Harturig, E. Wiener-Aunear, J. Smit, and S. P. S. Porto, *Phys. Rev. B*, **3**, 2078 (1971). [LO–TO = longitudinal optical–transverse optical and LA–TA = longitudinal acoustic–transverse acoustic.]

Table VIII. CO Stretching Valence Force Constants (K) and Geminal (i) and Indirect (j) Interaction Constants of $Ru_{3-x}Os_x(CO)_{12}$ ($x = 0, 1, 2, 3$)

		Ru_3-$(CO)_{12}$	Ru_2Os-$(CO)_{12}$	$RuOs_2$-$(CO)_{12}$	Os_3-$(CO)_{12}$
K_{eq}	Ru	16.641	16.626	16.619	
	Os		16.540	16.538	16.527
K_{ax}	Ru	16.673	16.687	16.694	
	Os		16.775	16.777	16.788
i_1 (i_{ee})	Ru	0.339	0.342	0.347	
	Os		0.363	0.375	0.376
i_2 (i_{aa})	Ru	0.399	0.402	0.420	
	Os		0.447	0.476	0.481
i_3 (i_{ea})	Ru	0.233	0.237	0.238	
	Os		0.256	0.256	0.259
j_1	Ru-Ru	0.162	0.154		
	Ru-Os		0.189	0.177	
	Os-Os			0.195	0.189
j_2	Ru-Ru	0.125	0.117		
	Ru-Os		0.123	0.119	
	Os-Os			0.109	0.104
j_3	Ru-Ru	0.069	0.022		
	Ru-Os		0.059	0.042	
	Os-Os			0.067	0.048
j_4	Ru-Ru	0.208	0.219		
	Ru-Os		0.230	0.213	
	Os-Os			0.288	0.251
j_5	Ru-Ru	0.008	0.0		
	Ru-Os		0.032	0.021	
	Os-Os			0.013	0.026
j_6	Ru-Ru	0.079	0.075		
	Ru(eq)-Os(ax)		0.074	0.076	
	Ru(ax)-Os(eq)		0.073	0.074	
	Os-Os			0.077	0.073
j_7	Ru-Ru	0.040	0.040		
	Ru(eq)-Os(ax)		0.037	0.036	
	Ru(ax)-Os(eq)		0.036	0.034	
	Os-Os			0.034	0.032

in Figure 6. Details of the methods of calculation are given in the Appendix.

It is a striking result obtained for this series of isostructural compounds that the *average* C–O stretching force constant has the same value (16.66 mdyn/Å) for all four compounds. Moreover, the means of the ruthenium-localized and osmium-localized C–O stretching force constants of the two mixed compounds have also the same values.

The characteristic differences of the forms of the spectra (regarding frequency distribution) are reflected in grosso modo by the trend (shown in Figure 6) of the C–O stretching force constants: that is, both the frequencies and the stretching constants "spread" while going from Ru_3 to Os_3. The spacing of the frequencies is governed, of course, not only by the principal K(C–O) constants but also by the interaction constants. We can see that *all* geminal interaction constants increase regularly (and their average does so linearly) when going from $Ru_3(CO)_{12}$ to $Os_3(CO)_{12}$, and consequently the spectra spread even more in this series than the K(C–O) pattern does.

This is in contrast with the Co_4- and $Rh_4(CO)_{12}$ pair of isostructural compounds,[4] where both spectra were spread in a comparable manner, but all the frequencies (and hence, of course, also their average) of the rhodium compound were higher. So far no similar study of trinuclear or higher nuclear clusters of analogous structures has been made, hence there are not yet enough data known for us to speculate on the systemization of such trends.

The indirect (vicinal "through space" or "through M–M bond") CO···C′O′ interactions cover the range between 0.02 and 0.25 mdyn/Å (all being positive), and they are usually higher the shorter the distance between the interacting groups.

The nonzero value of these interactions is important because it clearly demonstrates that any treatment based on local symmetry—that is, one that considers only geminal interaction constants—is completely invalid. The importance of indirect interactions was recognized in a qualitative way by Cotton and Wing[21] in their statement that "the question of the nature and magnitude of the interaction between the two $M(CO)_5$ halves of the $(CO)_5MM(CO)_5$ molecule or between the two $M(CO)_4L$ halves of an $L(CO)_4MM(CO)_4L$ molecule is an important and interesting one". In 1966 Lewis, Manning, and Miller[26] were first *uniquely* to determine numerical "interaction constants across a metal–metal bond" for a series of $(R_3P)_2Mn_2(CO)_8$ compounds. In spite of these and subsequent publications on di- and polynuclear carbonyls[27] indirect interactions have often deliberately been neglected[28] in order to reduce the number of parameters involved in vibrational analyses of "natural" (all-^{12}CO) IR spectra—analyses which are otherwise uniquely insoluble because they are underdetermined. However, it is fundamental requirement in vibrational spectroscopy that an acceptable force field fit the experimental data not only of the "natural abundance" compound but also of all its isotopic substitution products. For metal carbonyls it has been found that the "C–O-factored field" may excellently fulfil this requirement for ^{13}CO derivatives.[29-31] Kaesz et al.[32] and independently Cotton et al.[33] suggested what is now quite evident: that correct analyses must use isotopic data to reduce underdetermination. Setting indirect interaction constants to zero is not an acceptable alternative. The nonzero values of such interaction constants obtained in our refinement (when the calculated frequencies excellently match the spectra of both $M_3(^{12}CO)_{11}(^{13}CO)$ and $M_3(^{12}CO)_{12}$ species) underline the invalidity of the local symmetry approach for polynuclear metal carbonyls.

Table IX. N Matrix Elements and Rotational Parameters for Species E′

	Q_5	Q_6	Q_7
	$Ru_3(CO)_{12}$		
S_5	0.7493	−0.6287	−0.2079
S_6	0.6559	0.7479	0.1022
S_7	0.0912	−0.2130	0.9728
parameters: $\phi_1 = 40°$, $\phi_2 = 12°$, $\phi_3 = -6°$			
	$Os_3(CO)_{12}$		
S_5	0.8089	−0.5877	−0.0175
S_6	0.5801	0.8026	−0.1392
S_7	0.0958	0.1024	0.9901
parameters: $\phi_1 = 36°$, $\phi_2 = 1°$, $\phi_3 = 8°$			

The extent of coupling between the symmetry coordinates in the third-order species E′ is shown in Table IX in terms of N matrices. (The squares of the terms of these matrices are related to the potential energy distribution (PED) but we prefer the N-matrix presentation because the signs of the terms then

(26) J. Lewis, A. R. Manning, and J. R. Miller, *J. Chem. Soc. A*, 845 (1966).
(27) E.g.: (a) H. Haas and R. K. Sheline, *J. Chem. Phys.*, **47**, 2996 (1967); (b) P. S. Braterman, *J. Chem. Soc. A*, 2907 (1968); (c) F. Cariati, V. Valenti, and G. Zerbi, *Inorg. Chim. Acta*, **3**, 378 (1969); (d) G. Bor, *ibid.*, **3**, 196 (1969); (e) B. F. G. Johnson, J. Lewis, and P. W. Robinson, *J. Chem. Soc. A*, 2693 (1969); (f) A. R. Manning and J. R. Miller, *ibid.*, 3352 (1970).
(28) E.g.: (a) E. W. Abel, J. Dalton, I. Paul, J. G. Smith, and F. G. A. Stone, *J. Chem. Soc. A*, 1203 (1968); (b) F. T. Delbeke, E. G. Claeys, R. M. De Caluwe, and G. P. van der Kelen, *J. Organomet. Chem.*, **23**, 505 (1970); (c) F. T. Delbeke, E. G. Claeys, G. P. van der Kelen, and Z. Eechkaut, *ibid.*, **25**, 213 (1970); (d) E. O. Fischer, T. L. Lindner, F. R. Kreissl, and P. Braunstein, *Chem. Ber.*, **110**, 3139 (1977).
(29) R. N. Perutz and J. J. Turner, *Inorg. Chem.*, **14**, 262 (1975).
(30) G. Bor, G. Battiston, and G. Sbrignadello, *J. Organomet. Chem.*, **122**, 413 (1976).
(31) J. K. Burdett, M. Poliakoff, J. A. Timney, and J. J. Turner, *Inorg. Chem.*, **17**, 948 (1978).
(32) H. D. Kaesz, R. Bau, D. Hendrickson, and J. M. Smith, *J. Am. Chem. Soc.*, **89**, 2844 (1967).
(33) F. A. Cotton, A. Musco, and G. Yagupsky, *Inorg. Chem.*, **6**, 1357 (1967).

indicate the relative phase of the coupling of the three symmetry coordinates in this species.) The columns of the matrix **N** indicate the composition of the C–O stretching normal coordinates in terms of the corresponding symmetry coordinates. The correctness of the Huggins–Flitcroft–Kaesz assignment is shown by the fact that both in the triruthenium and in the triosmium case the diagonal terms dominate. With $Os_3(CO)_{12}$ all N_{ii} terms are higher than the corresponding values of the triruthenium compound which means that for $Os_3(CO)_{12}$ the extent of coupling is less than for $Ru_3(CO)_{12}$.

In the second column (coefficients for Q_6) there is a very important reversal of signs between Ru_3- and $Os_3(CO)_{12}$: symmetry coordinate S_7 is mixed in phase with the dominating S_6 for $Os_3(CO)_{12}$ whereas the corresponding coupling is out of phase for $Ru_3(CO)_{12}$. It is this difference in the sense of coupling between S_6 and S_7 which is responsible for the extremely low (relative) intensity of the 2018-cm^{-1} band of $Ru_3(CO)_{12}$ compared to that at 2015 cm^{-1} of $Os_3(CO)_{12}$.

A more thorough treatment of the IR band intensities, including a quantitative interpretation of the induced dipole moment contribution, is the subject of a separate paper.[34]

Our determination of the extent of coupling in the (IR inactive) species A_1' is only tentative. The approach suggested by Ernstbrunner and Kilner[35] could not even be tried since no solution Raman spectra could be obtained. Hence our only way to estimate the A_1' coupling was to rotate the **F** matrix of this species, after having fixed the IR-inactive frequencies and determined the E′ coupling, until all constants fell into the well-established regions found in previous studies. The coupling corresponds to $\phi(A_1') = 47$ and 55° for Ru_3- and $Os_3(CO)_{12}$, respectively. (For the significance of the ϕ values see the Appendix.) Since the maximum coupling in a second-order species corresponds to 45°, the estimated values point to a nearly complete coupling. Moreover, the numerical values (>45°) indicate an inversion relative to the initial assignment of the symmetry coordinates (Table VII). That is, the axial component contributes somewhat more to the higher (in phase) A_1' modes than the radial one. The opposite is true for the lower (out of phase) A_1' mode. This is in accord with the mixing in the E′ modes where the highest (in phase) vibration is also an axially dominated one. Finally, the fact that the coupling is less for $Os_3(CO)_{12}$ than for the ruthenium compound, also of species A_1', accords with the regularity observed for carbonyls of analogous structures: the coupling between different sets of C–O vibrators is near to the maximum when the different C–O stretching force constants are nearly equal, and this coupling is reduced when the difference between unequal K(C–O) constants is increased.

Experimental Section

$Ru_3(CO)_{12}$ and $Os_3(CO)_{12}$ (Alfa) were recrystallized from acetone before use. Mixed crystals of the two compounds were prepared by crystallization from acetone.

The mixed-metal clusters $RuOs_2(CO)_{12}$ and $Ru_2Os(CO)_{12}$ were prepared either by thermal reaction of $Os_3(CO)_{12}$ and $Ru_3(CO)_{12}$ in xylene[18a] or by reacting $Ru_2(CO)_6Cl_4$ with OsO_4 under CO pressure.[18c] Both methods give rise to a mixture of the four species in a nearly statistical ratio (1:2:2:1). All four compounds have very similar physical and chemical properties and their separation is not trivial. No method has been described in the literature for this separation, and so we describe in some detail the method we employed.

The reaction solution was filtered and the solvent removed from the filtrate. The solid residue was extracted with $CHCl_3$, giving a yellow solution which was deposited on 20 × 40 thin layer chromatography plates. The adsorbate, silica gel (Merck $PF_{254+336}$), was of 1-mm thickness. The eluant was petroleum ether containing 5% cyclohexane. Not more than 0.5 mL of nearly saturated $CHCl_3$ solution was used for each plate, corresponding to ca. 1 mg of mixture. The elution time was 5–6 h. The compounds move toward the top of the plate in the order $Ru_3 > Ru_2Os > RuOs_2 > Os_3$. In general, one elution does not enable a complete separation, as a broad yellow band is initially obtained. The band was divided into four roughly equal strips from which the crude compound was extracted by $CHCl_3$. The same procedure was repeated, collecting together samples with similar composition (vide infra) until complete purification had been achieved. Clearly, a fundamental part of the separation is the monitoring of the composition of intermediate samples. This was performed in three different ways.

(a) The best check is provided by the solid-state Raman spectrum in the 150–200-cm^{-1} region. Each complex exhibits in this region a strong band, assigned to a totally symmetric M–M stretching vibration, which lies at 187 cm^{-1} for Ru_3, at 179 cm^{-1} for Ru_2Os, at 171 cm^{-1} for $RuOs_2$, and at 160 cm^{-1} for Os_3.[16] The bands are well resolved, and their relative intensity is roughly proportional to the percentage composition of the samples.

(b) The second method is to measure the frequency of the strongest IR ν(CO) solution band. In CCl_4, where all complexes are quite soluble, this band appears at 2066 cm^{-1} for Os_3, at 2063 cm^{-1} for $RuOs_2$, at 2060 cm^{-1} for Ru_2Os, and at 2058 cm^{-1} for Ru_3. The bands are not resolved in the solutions of mixtures, but they appear as a unique band, which moves from 2058 to 2066 cm^{-1} as the average content of Ru decreases and that of Os increases. A plot of the frequency of this band for the pure compounds against Os:Ru content is linear. By interpolation, one can approximately calculate the average composition of a mixture in terms of Os:Ru ratio and, where the mixture contains only two known complexes, their relative percentage may be obtained.

(c) The least suitable method is to observe the mass spectra of the samples. These data are less conclusive, as the intensity of the peaks is not proportional to composition and the isotopic patterns of the molecular ions are very complicated. However, this method is a very convenient way of checking the absence of high molecular weight impurities.

^{13}CO enrichment was performed in a pressure-tested glass ampule. Saturated hexane solutions (ca. 3 mL) of the homonuclear dodecacarbonyls were placed (at room temperature) under 1 atm of a very large excess of 5% (or 13%) of ^{13}CO (Merck Sharp and Dohme) diluted with 95% (or 87%, respectively) of regular carbon monoxide. Light was carefully excluded in order to avoid photochemical formation of $Ru(CO)_5$. Ligand-exchange equilibrium was approached within 24 h at 52 °C for $Ru_3(CO)_{12}$ and within 72 h at 100 °C for $Os_3(CO)_{12}$, respectively, in accord with ^{14}CO-exchange experiments reported by Cetini et al.[36]

On the assumption of a statistical distribution of isotopically labeled CO in the dodecacarbonyls, there will be 34% of the monosubstituted species in the 5%-enriched sample. This is close to the maximum statistically possible relative concentration of 38.5%. We preferred to work at the 34% level because there the amount of di- and especially polysubstituted dodecacarbonyls is still negligible (Figure 19). At 13% ^{13}CO ligand content there is again ca. 34% of the monosubstituted species, but 28% of the disubstituted and 14% of the trisubstituted dodecacarbonyls are to be expected. Hence, the additional exchange experiment involving 13% of ^{13}CO served the purpose of sorting out bands belonging to polysubstituted species and in addition permitted a semiquantitatively check on whether equilibrium between the gas phase and dissolved carbonyl has been achieved (since no independent analysis of the ^{13}CO content of the enriched samples was performed).

Solution and KBr pellet IR spectra of the pure homo- and heterotrinuclear dodecacarbonyls were scanned with a Perkin-Elmer Model 325 spectrometer. The slit program used (4.5) corresponded to a spectral slit width of ca. 1.0 cm^{-1} at 2000 cm^{-1} and to ca. 2 cm^{-1} at 4000 cm^{-1}. Hexane (spectroscopic quality, Merck AG) was used as solvent for the C–O stretching and the 600–200-cm^{-1} region while CCl_4 was used for the overtone region around 4000 cm^{-1}. CaF_2 cells of 2-mm thickness were used, without solvent compensation, for this latter region; NaCl cells (0.2–1-mm thickness) with solvent compensation were used to obtain the ν(CO) spectra.

The high precision (±0.2 cm^{-1}) C–O stretching spectra were scanned with 5- or 10-fold wavenumber scale expansion (1 cm on the chart

(34) G. A. Battiston, G. Sbrignadello, and G. Bor, *Inorg. Chem.*, following paper in this issue.
(35) E. E. Ernstbrunner and M. Kilner, *J. Chem. Soc., Dalton Trans.*, 2598 (1975).
(36) G. Cetini, O. Gambino, E. Sappa, and G. A. Vaglio, *Atti Accad. Sci. Torino, Cl. Sci. Fis., Mat. Nat.*, **101**, 855 (1967).

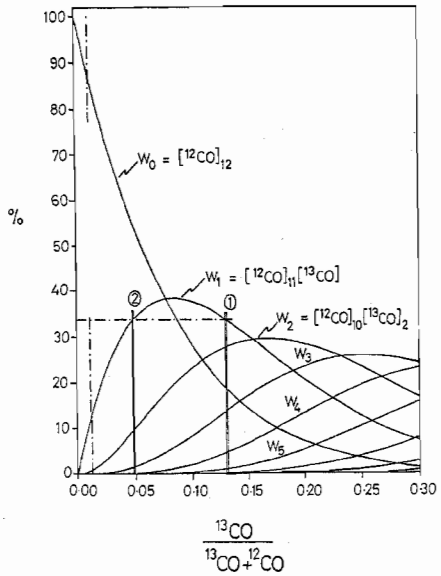

Figure 19. Variation of concentration of isomeric ^{13}CO-contained species of $M_3(CO)_{12}$ as a function of the fraction of ^{13}CO to total CO. For comments on the ^{13}CO concentrations labeled 1 and 2, see the text.

Table X. Symmetry Force Constants (F Matrix Elements) of the $M_3(CO)_{12}$ Compounds (D_{3h})

A_1'	$F_{11} = K_{eq} + i_1 + j_1 + j_2 + 2j_3$
	$F_{22} = K_{ax} + i_2 + 2j_4 + 2j_5$
	$F_{12} = 2(i_3 + j_6 + j_7)$
A_2'	$F_{33} = K_{eq} - i_1 - j_1 - j_2 + 2j_3$
A_2''	$F_{44} = K_{ax} - i_2 + 2j_4 - 2j_5$
E'	$F_{55} = K_{ax} + i_2 - j_4 - j_5$
	$F_{66} = K_{eq} + i_1 - (j_1 + j_2)/2 - j_3$
	$F_{77} = K_{eq} - i_1 + (j_1 + j_2)/2 - j_3$
	$F_{56} = 2i_3 - j_6 - j_7$
	$F_{57} = 3^{1/2}(j_6 - j_7)$
	$F_{67} = (3^{1/2}/2)(j_1 - j_2)$
E''	$F_{88} = K_{ax} - i_2 - j_4 + j_5$

Table XI. C–O Stretching Valence Force Constants and Geminal (i) and Indirect (j) Interaction Constants of $M_3(CO)_{12}$ Compounds Expressed in Terms of the Symmetrized F_{ij} Elements

$$K_{eq} = (F_{11} + F_{33} + 2F_{66} + 2F_{77})/6$$
$$K_{ax} = (F_{22} + F_{44} + 2F_{55} + 2F_{88})/6$$
$$i_1 = (F_{11} - F_{33} + 2F_{66} - 2F_{77})/6$$
$$i_2 = (F_{22} - F_{44} + 2F_{55} - 2F_{88})/6$$
$$i_3 = (F_{12} + 2F_{56})/6$$
$$j_1 = (F_{11} - F_{33} - F_{66} + F_{77} + 2(3^{1/2})F_{67})/6$$
$$j_2 = (F_{11} - F_{33} - F_{66} + F_{77} - 2(3^{1/2})F_{67})/6$$
$$j_3 = (F_{11} + F_{33} - F_{66} - F_{77})/6$$
$$j_4 = (F_{22} + F_{44} - F_{55} - F_{88})/6$$
$$j_5 = (F_{22} - F_{44} - F_{55} + F_{88})/6$$
$$j_6 = (F_{12} - F_{56} + 3^{1/2}F_{57})/6$$
$$j_7 = (F_{12} - F_{56} - 3^{1/2}F_{57})/6$$

= 5 or 2.5 cm^{-1}); 2- to 10-fold ordinate expansion was used for the weak satellites. The same type of expansion was used also in the 4000-cm^{-1} region, where even a CCl_4 solution saturated at 35 °C and scanned with a 2-mm cell yielded only very weak absorptions. The low solubility of Ru_2Os-, $RuOs_2$-, and $Os_3(CO)_{12}$ prevented the study of the 4000-cm^{-1} region for these compounds.

Raman spectra were recorded at room temperature on a Spex 1401 spectrometer with red-enhanced optics using the 6471-Å line of a Spectra Physics A/Kr laser at ca. 20-mW incident intensity. Spectral slit widths were generally 2 cm^{-1} and occasionally 1.5 cm^{-1}.

Acknowledgment. We are indebted to the Royal Society and NATO (S.F.A.K. and P.L.S.), to the British Council and CNR (P.L.S. and R.R.), and to the Schweizerischer Nationalfonds zur Förderung der wissenschaftlichen Forschung (G.B., under Grant No. 2.902-0.77) for support.

Appendix

Force Constant Calculations. The principles of our "rotational parameter" method (Braterman[2b] uses the term "independent variable" method for the approach published previously by one of us[37]) were given in some of our earlier papers.[4,20,38] Therefore here we refer, in part, to those publications. However in the present paper we should like to describe the calculational procedure in a way which will permit its facile application by other workers.

(A) $M_3(CO)_{12}$ Complexes (D_{3h}). Two different methods of calculation on two different levels of refinement were used, one after the other.

(1) First, in several separate cycles the approximate force constants were estimated, and the nearly final assignment was checked by the following procedure.

Approximate initial values were estimated for the C–O stretching force and interaction constants by transferring values from known model compounds; these initial (approximate) constants were arranged in a (symmetric) 12 × 12 force constant matrix $\mathbf{f}^{(a)}$ (approximate K(C–O) force constants as diagonal elements $f_{ii}^{(a)}$ and approximate interaction constants between the ith and jth ligand as off-diagonal elements $f_{ij}^{(a)}$). $\mathbf{f}^{(a)}$ was then diagonalized by a computer procedure yielding the diagonal matrix $\mathbf{Y}^{(a)}$ whose elements $y_i^{(a)}$ are connected with the approximate (i.e., calculated in this step a) C–O stretching frequencies through eq 1.[37] (At this level degen-

$$y_i^{(a)} = \lambda_i^{(a)}/\mu_{CO} = 0.40407 \times 10^{-5}(\nu_i^{(a)})^2 \qquad (1)$$

erate frequencies appear twice in the $\mathbf{Y}$ matrix.) The computer diagonalization procedure delivers also the corresponding (approximate) orthonormal eigenvalue matrix $\mathbf{n}^{(a)}$, since

$$\tilde{\mathbf{n}}^{(a)}\mathbf{f}^{(a)}\mathbf{n}^{(a)} = \mathbf{Y}^{(a)} \qquad (2)$$

where $\tilde{\mathbf{n}}$ is the transposition of $\mathbf{n}$ and, since $\mathbf{n}$ is orthonormal, $\tilde{\mathbf{n}} = \mathbf{n}^{-1}$. For completion of one cycle of refinement, the matrix $\mathbf{n}^{(a)}$, belonging to the first approximation of force constants, was applied to the diagonal matrix $\mathbf{Y}^{(t)}$ which contains the true (experimental) frequencies (i.e., the $y_i^{(t)}$ values derived according to eq 1 from the experimental $\nu_i^{(t)}$ values, as far as they were known at that stage, and otherwise from best possible estimations). An "inverse diagonalization step", eq 3,

$$\mathbf{n}^{(a)}\mathbf{Y}^{(t)}\tilde{\mathbf{n}}^{(a)} = \mathbf{f}^{(b)} \qquad (3)$$

yielded a second approximate force constant matrix $\mathbf{f}^{(b)}$. If the assignment was correct, we usually got a convergence toward reasonable force constant values. If, however, the force constants obtained in $\mathbf{f}^{(b)}$ were less acceptable than the initial ones in $\mathbf{f}^{(a)}$, this was in most cases an indication of an incorrect assignment.

In an "isotopic procedure" which is also included in our computer program the frequencies of the mono-^{13}CO-substituted derivatives were calculated according to the principles given in eq 5, 7, 7a, and 11 of ref 38: the isotopic mass effect is (deliberately) transferred from matrix $\mathbf{G}$ onto the force constant matrix $\mathbf{f}$ leaving $\mathbf{G}$ unaffected by isotopic substitution and still defined as $\mathbf{G}^{-1} = (1/\mu)\mathbf{E}$ according to the Cotton–Kraihanzel principle.[39] For this purpose all the elements of the column and the line of matrix $\mathbf{F}$, corresponding to a required position of the ^{13}CO ligand, were multiplied by $[\mu(^{13}CO)/\mu(^{12}CO)]^{1/2} = 0.977\,27$ to yield the "isotopic" force constant matrix $\mathbf{f}^{(i)}$ which was then diagonalized in the usual way. By applying eq 1, we calculated the ^{13}CO stretching frequencies of the chosen mono-^{13}CO-substituted molecule.

(37) G. Bor, *Inorg. Chim. Acta*, **1**, 81 (1967).
(38) G. Bor, *J. Organomet. Chem.*, **10**, 343 (1967).
(39) F. A. Cotton and C. S. Kraihanzel, *J. Am. Chem. Soc.*, **84**, 4432 (1962).

Corrections of the assignments (mainly of the IR-inactive modes) could be performed also on this level. Such corrections were based on the observed and calculated isotopic bands. $\mathbf{f}^{(b)}$ values were adjusted and assignments changed according to need, and the next cycle was started by diagonalizing $\mathbf{f}^{(b)}$, yielding $\mathbf{Y}^{(b)}$ and $\mathbf{n}^{(b)}$.

Two to three cycles of such one-step refinements yielded the principally correct assignment (correct sequence of frequencies), together with matrix $\mathbf{n}^{(c)}$ containing the "correct" eigenvectors. These formed the basis for the second level of refinement.

(2) On this second level the further refinement (of the calculated isotopic frequencies and of the force constants) was performed by the principle of matrix rotation. In order to perform these rotations, we transformed to a symmetrical basis; i.e., we substituted the 12th-order **f** matrix by several **F** matrices according to[40] eq 4, where **U** is the matrix of the or-

$$\mathbf{F} = \mathbf{U}\mathbf{f}\tilde{\mathbf{U}} \tag{4}$$

thogonal transformation from internal to symmetry coordinates. For the $M_3(CO)_{12}$ (D_{3h}) compounds the expressions for F_{ij} elements vs. valence force constants f_{ij} are given in Table X. The A_1' species is doubly occupied by C–O stretching symmetry coordinates, whereas species E′ is triply occupied. Hence $\mathbf{F}^{(A_1')}$ is a second-order and $\mathbf{F}^{(E')}$ is a third-order symmetric matrix. The **F** matrices for the other three symmetry species (A_2', A_2'', and E″) contain only one F_{ii} element since they are only singly occupied. Hence these species do not participate in the "rotational" refinement. In the same way the orthogonal matrix **n** reduces to blocks **N** of second (A_1') and third order (E′), respectively, as symmetry is introduced according to eq 5. (The symmetry-reduced matrices **N** have

$$\mathbf{N} = \mathbf{U}\mathbf{n} \quad \text{and} \quad \tilde{\mathbf{N}} = \tilde{\mathbf{n}}\tilde{\mathbf{U}} \tag{5}$$

the property of connecting the vectors constructed from symmetry coordinates (S) with the normal coordinates (Q) according to $S = \mathbf{N}Q$.)

The **F** matrices of the second- and third-order species were diagonalized by matrices **N** to yield appropriate matrices **Y** according to eq 6. The original 12th-order matrix **Y** related

$$\tilde{\mathbf{N}}\mathbf{F}\mathbf{N} = \mathbf{Y}^{(\text{species})} \tag{6}$$

to **f** and **n** is split into several "submatrices": one of second order $\mathbf{Y}^{(A_1')}$ related to the second-order species A_1' and containing the two (original) elements y_1 and y_2 (i.e., the two roots of $\mathbf{F}^{(A_1')}$), one of third order $\mathbf{Y}^{(E')}$ related to the third-order species E′ and containing the three (original) elements y_5, y_6, and y_7 (i.e., the three roots of $\mathbf{F}^{(E')}$), and, of course, three first-order terms related to the three first-order species A_2', A_2'', and E″, where obviously $\mathbf{F} = F_{ii} = y_i$ (i = 3, 4, 8). The sum of the orders of the **F** blocks is thus only 8, since the two components of the doubly degenerate species E′ and E″ are identical, and so one of each is redundant in this treatment.

The initial numerical compositions of $\mathbf{N}^{(A_1')}$ and $\mathbf{N}^{(E')}$ for the second level of refinement were obtained from $\mathbf{n}^{(c)}$ through eq 5. Then the rotational matrix character of the matrices **N** was exploited. For species A_1' we have the form (7) where

$$\mathbf{N}^{(A_1')} = \begin{bmatrix} \cos\phi_A & -\sin\phi_A \\ \sin\phi_A & \cos\phi_A \end{bmatrix} \tag{7}$$

ϕ_A is the rotational parameter for species A_1'.[41] The third-order rotational matrix $\mathbf{N}^{(E')}$ was obtained according to conventions given in eq 9–11 of ref 4 and is explicitly given in terms of three rotational parameters ϕ_1, ϕ_2, and ϕ_3 in Table IV of ref 4. An initial value for $\phi_A(A_1')$ was calculated from $N_{11}^{(A_1')}$ ($=N_{22}$) = cos $\phi_A(A_1')$, while the initial values of ϕ_1 to ϕ_3 (E′) were obtained from $\mathbf{N}^{(E')}$ as described on p 821 of ref 4. All four rotational parameters were then varied in both directions around their initial values, and to each set the principal equation (8) was applied. In practice, for every set

$$\mathbf{N}\mathbf{Y}\tilde{\mathbf{N}} = \mathbf{F} \tag{8}$$

of the four rotational parameters the F_{ij} elements were calculated according to eq 9 (n = 2 for A_1' and n = 3 for E′).

$$F_{ij} = \sum_{k=1}^{n} N_{ik}N_{jk}y_k \tag{9}$$

The values for F_{ij} thus obtained for the species A_1' and E′ were then combined with the F_{ii} values of species A_2', A_2'', and E″ (which are constant, as long as the corresponding $\nu_3(A_2')$, $\nu_4(A_2'')$, and $\nu_8(E'')$ are not changed), according to the equations given in Table XI, to yield the valence force and interaction constants belonging to every set of values for the rotational parameters ϕ_A and ϕ_1–ϕ_3.

These force constants were now again arranged into a matrix **f** of 12th order, corresponding to the molecular symmetry D_{3h}. Isotopic frequencies were calculated on this basis also as outlined above for the first level of refinement.

Five out of the eight frequencies (ν_1 and ν_4–ν_7) were known exactly, and the assignment of ν_1, ν_6, and ν_7 was unambiguous from the beginning. The correct assignment of ν_4 and ν_5 was soon decided (see Discussion). ν_2, ν_3, and ν_8 were not known exactly and had to be varied in small steps until a perfect agreement with the observed isotopic frequencies, and, at the same time, a "good" set of force and interaction constants had been obtained.

(B) $M_2M'(CO)_{12}$ Complexes (C_{2v}). In this reduced symmetry the distribution of the 12 C–O stretching modes among the irreducible representations of point group C_{2v} is

$$\Gamma(CO) = 5\ A_1 + 1\ A_2 + 4\ B_1 + 2\ B_2$$

The presence of a fifth-, a fourth-, and a second-order species would demand the use of 17 rotational parameters, and hence it would be hardly practicable to use our second-level refinement techniques. Moreover, due to the extremely small quantities of the samples Ru_2Os- and $RuOs_2(CO)_{12}$ available, no isotopic enrichment has yet been possible. Without good quality spectra of isotopically enriched samples these molecular vibrational problems are highly underdetermined: there are 4 C–O stretching force constants for each of these compounds and 6 geminal plus 16 indirect interaction constants.

Therefore only the approach described in part 1 of the Appendix was applied for the mixed compounds. With refinement cycles, based on the principle of eq 3, the force constants (which build up matrices $\mathbf{f}^{(a)}$ and $\mathbf{f}^{(b)}$ in eq 2 and 3, respectively) were improved in small steps, until every pair of its initial and refined values did not show a difference of more than 0.002 mdyn/Å. In the final results only one interaction constant came close to this limit, whereas for the other constants the change during the last refinement cycle was around 0.0005 mdyn/Å.

Although the force and interaction constants converged smoothly to the results shown in Figure 6 and Table VIII and although these are quite convincing (and also aesthetically attractive because of their symmetry), it must be admitted that

(40) A. G. Meister and F. F. Cleveland, *Am. J. Phys.*, **14**, 13 (1946).
(41) The rotational "independent" parameter ϕ has been first introduced, for $XM(CO)_5$ compounds, by Braterman, Bau, and Kaesz,[42] and it is related to the parameter introduced independently by one of us[37] by $\beta = 2\phi$. The parameters ρ and p used by Manning and Miller[43] for the case of $XM(CO)_5$ complexes are then ρ = tan ϕ and p = tan 2ϕ = tan β.
(42) P. S. Braterman, R. Bau, and H. D. Kaesz, *Inorg. Chem.*, **6**, 2097 (1967).
(43) A. R. Manning and J. R. Miller, *J. Chem. Soc. A*, 1521 (1966).

the "final" set of force and interaction constants did not give as good an agreement with the few and poorly resolved natural isotopic bands as was the case for the homo-trinuclear compounds: instead of an agreement within ±0.3 cm^{-1} between calculated and observed isotopic bands for $M_3(CO)_{12}$ complexes, there was sometimes a discrepancy of as much as 2 cm^{-1} for the mixed compounds.

Registry No. $Ru_3(CO)_{12}$, 15243-33-1; $Ru_2Os(CO)_{12}$, 12389-47-8; $RuOs_2(CO)_{12}$, 12389-50-3; $Os_3(CO)_{12}$, 15696-40-9; $Ru_3(^{12}CO)_{11}(^{13}CO)$ (eq isomer), 73295-93-9; $Ru_3(^{12}CO)_{11}(^{13}CO)$ (ax isomer), 73346-53-9; $Os_3(^{12}CO)_{11}(^{13}CO)$ (eq isomer), 73295-94-0; $Os_3(^{12}CO)_{11}(^{13}CO)$ (ax isomer), 73346-54-0.

Contribution from the Laboratory for the Chemistry and Technology of the Radioelements of CNR, I-35100 Padua, Italy, and the Department of Industrial and Engineering Chemistry of the Swiss Federal Institute of Technology, ETH, CH-8092 Zurich, Switzerland

Infrared Spectroscopic Studies on Metal Carbonyl Compounds. 23.[1a] A Simple Quantitative Treatment of the Infrared Band Intensity and the Induced Metal–Metal Dipole Contribution to It in Polynuclear Metal Carbonyls. An Application to the Spectrum of $Ru_3(CO)_{12}$ and $Os_3(CO)_{12}$ in the Carbon–Oxygen Stretching Region

GIOVANNI A. BATTISTON,*[1b] GINO SBRIGNADELLO,[1b] and GYÖRGY BOR[1c]

Received September 7, 1979

The use of the spectra of ^{13}CO-enriched species to determine the extent of coupling between axial and equatorial C–O stretching symmetry coordinates for species E′ of the $M_3(CO)_{12}$ (M = Ru, Os) molecules with D_{3h} symmetry permits a quantitative study of the relative IR band intensities. A simple treatment is presented which considers not only the local oscillating CO dipoles but also the contribution of the dipole moment induced at the electronic centers on the metal atoms. It is assumed that the induced dipole moment is a linear function of the eigenvectors and that it can have the same *or opposite* direction with respect to the resultant of the local vibrating CO dipoles, giving rise to an increase or a decrease in the expected intensity. The observed intensity anomaly in the (C–O stretching region of the) IR spectrum of $Ru_3(CO)_{12}$, as compared with that of $Os_3(CO)_{12}$, which seems to contradict the analogous structures, can be explained by this simple treatment. The following numerical values, relative to the axial dipole moment gradient ($\mu_{ax}' = 1.0$), have been obtained: $\mu_{eq}' = 0.83$ (Ru) and 0.97 (Os); $\mu_M' = 0.83$ (Ru) and 0.68 (Os), where μ_M' is the gradient of the induced M–M dipole. The treatment is generally applicable for other types of di- and polynuclear metal carbonyls.

Introduction

The fundamentals of the interpretation and prediction of the infrared band intensities of simple mononuclear metal carbonyl derivatives have been given by Orgel[2] and by El-Sayed and Kaesz.[3] These treatments based on the local oscillating dipoles have been later enriched by contributions of Bigorgne et al.,[4] Lewis, Manning and Miller,[5] Abel and Butler,[6] Beck et al.,[7] Wing and Crocker,[8] Haas and Sheline,[9] and others.[10] The quantitative interpretation of the intensities is fundamentally related to the exact determination of the extent of coupling between the axial and radial types of CO sets.[11] In this direction a very important step was made by Kaesz et al.[12] and independently by Cotton et al.[13] in introducing the use of isotopically substituted molecules to make the force field more determinate. The most important further refinement, introduced by Braterman, Bau, and Kaesz[14] for $XM(CO)_5$ (M = Mn, Re), was then the recognition that the dipole moment gradients are generally not equal for different sets of C–O vibrators. Moreover, another additional term has been introduced by Darensbourg and Brown[15] to account for the intensity contribution arising from the vibration of a dipole induced by the in-phase vibration of all CO groups of a $LM(CO)_5$ derivative, where a charge is created on the central metal atom, which is then compensated by an electron flow along the L–M bond. This type of intensity enhancing effect was first predicted (as "electronic migration" along the M–L axis) by Orgel[2] and considered as "synergic motion of electrons on the axis" also by Braterman et al.;[14] it is called also "vibronic contribution"[15] or "orbital following effect".[10c] Also our own analysis[16] of the $Me_3EFe(CO)_4$ (E = N, P, As, Sb, Bi) series dealt with a possible increase of the intensity of the highest frequency band by the contribution of an induced dipole along the E–Fe axis. Darensbourg introduced subsequently the concept of the "vibronic contribution" also into the analysis of the intensities of the $X_3EM(CO)_4$ type with C_{3v} symmetry[17] and later presented an extensive compilation based upon an extended set of data.[18]

The hypothesis that an intensity contribution from an induced dipole moment in the metal–metal direction can be

(1) (a) Previous paper of this series: ref 24. (b) Laboratory for the Chemistry and Technology of the Radioelements, CNR. (c) Department of Industrial and Engineering Chemistry of the Swiss Federal Institute of Technology.
(2) L. E. Orgel, *Inorg. Chem.*, **1**, 25 (1962).
(3) M. A. El-Sayed and H. D. Kaesz, *J. Mol. Spectrosc.*, **3**, 310 (1962).
(4) (a) A. Reckziegel and M. Bigorgne, *J. Organomet. Chem.*, **3**, 341 (1965); (b) O. Kahn and M. Bigorgne, *ibid.*, **10**, 137 (1967).
(5) J. Lewis, A. R. Manning, and J. R. Miller, *J. Chem. Soc. A*, 845 (1966).
(6) E. W. Abel and I. S. Butler, *Trans. Faraday Soc.*, **63**, 45 (1967).
(7) W. Beck, A. Melnikoff, and R. Stahl, *Chem. Ber.*, **99**, 3721 (1966).
(8) R. M. Wing and D. C. Crocker, *Inorg. Chem.*, **6**, 289 (1967).
(9) H. Haas and R. K. Sheline, *J. Inorg. Nucl. Chem.*, **29**, 693 (1967).
(10) For reviews on infrared intensities of metal carbonyls see: (a) L. M. Haines and M. H. B. Stiddard, *Adv. Inorg. Chem. Radiochem.*, **12**, 52, 89–100 (1969); (b) S. F. A. Kettle and I. Paul, *Adv. Organomet. Chem.*, **10**, 199 (1972); (c) P. S. Braterman, *Struct. Bonding (Berlin)*, **26**, 1 (1976).
(11) G. Bor, *Inorg. Chim. Acta*, **1**, 81 (1967); **3**, 191 (1969).
(12) H. D. Kaesz, R. Bau, D. Hendrickson, and S. Smith, *J. Am. Chem. Soc.*, **89**, 2844 (1967).
(13) F. A. Cotton, A. Musco, and G. Yagupski, *Inorg. Chem.*, **6**, 1357 (1967).
(14) P. S. Braterman, R. Bau, and H. D. Kaesz, *Inorg. Chem.*, **6**, 2097 (1967).
(15) D. J. Darensbourg and T. L. Brown, *Inorg. Chem.*, **7**, 959 (1968).
(16) G. Bor and M. Bigorgne, unpublished results, 1968.
(17) D. J. Darensbourg, *Inorg. Chim. Acta*, **4**, 597 (1970).
(18) D. J. Darensbourg, H. H. Nelson, and C. L. Hyde, *Inorg. Chem.*, **13**, 2135 (1974).

0020-1669/80/1319-1973$01.00/0